Associated production of the Higgs boson and a single top quark at hadron colliders

F. Maltoni, K. Paul, T. Stelzer, and S. Willenbrock
Department of Physics, University of Illinois at Urbana-Champaign, 1110 West Green Street, Urbana, Illinois 61801
(Received 28 June 2001; published 11 October 2001)

We study the production of the Higgs boson in association with a single top quark at hadron colliders. The cross sections for the three production processes (t channel, s channel, and W associated) at both the Fermilab Tevatron and the CERN Large Hadron Collider (LHC) are presented. We investigate the possibility of detecting a signal for the largest of these processes, the t-channel process at the LHC, via the Higgs boson decay into $b\bar{b}$. The QCD backgrounds are large and difficult to curb, hindering the extraction of the signal. Extensions of our analysis to the production of supersymmetric Higgs bosons are also addressed. The cross section is enhanced for large values of $\tan\beta$, increasing the prospects for extracting a signal.

DOI: 10.1103/PhysRevD.64.094023 PACS number(s): 13.85.Qk, 12.38.Bx, 14.65.Ha, 14.80.Bn

I. INTRODUCTION

The discovery of the Higgs boson as the culprit for electroweak symmetry breaking (EWSB) is one of the most challenging goals of present and future high-energy experiments. Within the standard model (SM), the mass of the Higgs boson is basically unconstrained with an upper bound of $m_h \lesssim 600-800$ GeV [1]. However, present data from precision measurements of electroweak quantities favor a moderate mass ($113\ \text{GeV} < m_h \lesssim 200-230\ \text{GeV}$) [2]. In addition, the minimal supersymmetric version of the SM (MSSM), which is one of its most popular extensions, predicts a Higgs boson with an upper mass bound of about 130 GeV [3–5]. Thus the scenario with an intermediate-mass Higgs boson ($113\ \text{GeV} < m_h \lesssim 130\ \text{GeV}$) is both theoretically plausible and well supported by the data.

Detailed studies performed for both the Fermilab Tevatron and the CERN Large Hadron Collider (LHC) (see, for example, Refs. [6] and [7], respectively) have shown that there is no single production mechanism or decay channel that dominates the phenomenology over the intermediate-mass range for the Higgs boson. Associated production of Wh or Zh [8] and $t\bar{t}h$ [9,10], with the subsequent decay $h\to\gamma\gamma$ [11–13] and $h\to b\bar{b}$ [14–18], are presently considered the most promising reactions to discover an intermediate-mass Higgs boson at both the Tevatron and the LHC. In this case one of the top quarks or the weak boson present in the final state can decay leptonically, providing an efficient trigger. The major difficulties in extracting a reliable signal from either of these two channels are the combination of a small signal and the need for an accurate control of all the background sources. In this respect, it would be useful to have other processes that could raise the sensitivity in this range of masses.

In this paper we re-examine the production of a Higgs boson in association with a single top quark (th production) at hadron colliders [19–22].[1] This process can be viewed as a natural extension of the single top production processes [23–28], where a Higgs boson is radiated off the top or off the W that mediates the bottom-to-top transition. As in the usual single-top production, the three processes of interest are characterized by the virtuality of the W boson in the process: (i) t channel (Fig. 1), where the spacelike W strikes a b quark in the proton sea, promoting it to a top quark; (ii) s channel (Fig. 2), where the W is timelike; (iii) W associated (Fig. 3), where there is emission of a real W boson.

There are two reasons *a priori* that make the above processes worthy of attention. The first one is that, based on simple considerations, one would expect Higgs boson plus single top production to be relevant at the Tevatron and at the LHC. While top quarks will be mostly produced in pairs via the strong interaction, the cross section for single top, which is a weak process, turns out to be rather large, about one-third of the cross section for top pair production [29,30]. If a similar ratio between $\sigma(th)$ and $\sigma(t\bar{t}h)$ is assumed, it is natural to ask whether th production could be used together with Wh, Zh, and $t\bar{t}h$ as a means to discover an intermediate-mass Higgs boson at the LHC. With this aim, the t-channel process has been previously considered when the Higgs boson decays into a pair of photons, with the result that too few events of this type would be produced, even at high-luminosity runs, at the LHC [20–22]. Since the dominant decay mode of the Higgs boson in this mass region is into $b\bar{b}$ pairs, this suggests searching for it using one or more b tags, in the same way as the $t\bar{t}h$ analysis is conducted. This possibility is pursued in the present paper.

The second reason for considering Higgs boson plus single top quark production is that it gives a rather unique possibility for studying the relative sign between the coupling of the Higgs boson to fermions and to vector bosons [22,31]. Measurements of Wh and $t\bar{t}h$ production rates test,

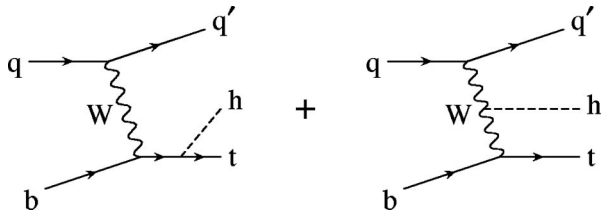

FIG. 1. Feynman diagrams contributing to the t-channel production of a Higgs boson plus a single top quark.

[1] We always understand th to include both top quark and top antiquark production.

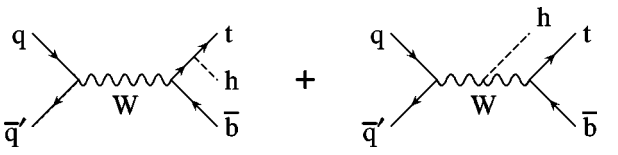

FIG. 2. Feynman diagrams contributing to the *s*-channel production of a Higgs boson plus a single top quark.

respectively, the Higgs boson coupling to the W and the Yukawa coupling to the top, but they cannot give any information on the relative sign between the two. In the th case, the t-channel and the W-associated (s-channel) cross sections depend strongly on the destructive (constructive) interference between the contributions from the Higgs boson radiated off the top and off the W boson. A measurement of the total rate for production of Higgs boson plus single top would therefore provide additional information on the EWSB sector of the SM.

As will be shown in detail in the following, at the Tevatron, the cross section for producing a Higgs boson in association with single top is of the order of 0.1 fb and therefore out of the reach of run II ($\lesssim 15\ \mathrm{fb}^{-1}$). On the other hand, with a cross section of the order of 100 fb, several thousands of events will be produced at the LHC with 30 fb^{-1}. Whether this will be enough to obtain a visible signal is the subject of the present investigation. As we will see, the number of signal events left after branching ratios, cuts, and efficiencies are taken into account is not large, and there are several backgrounds, both irreducible and reducible, to consider.

This paper is organized as follows. In Sec. II we present the leading-order results for Higgs boson plus single top production at both the Tevatron and the LHC, for the three channels mentioned above. The cross sections for the s-channel and W-associated processes, as well as for the t-channel process at the Tevatron, have not been presented before; we confirm the t-channel cross section at the LHC calculated in Refs. [20–22]. We investigate, in some detail, the interference in the various channels. Section III contains a study of signal and background for the t-channel production at the LHC, with both three and four b tags. Results on the t-channel production at the LHC in the minimal supersymmetric standard model (MSSM) are discussed in Sec. IV. We present our conclusions in the last section.

II. CROSS SECTIONS

There are three channels for the production of a Higgs boson plus a single top at hadron colliders:

$$\begin{aligned} &t \text{ channel} && qb \to q'th && \text{(Fig. 1)},\\ &s \text{ channel} && q\bar{q}' \to \bar{b}th && \text{(Fig. 2)},\\ &W \text{ associated} && gb \to W^- th && \text{(Fig. 3)}. \end{aligned}$$

In each case, the Higgs boson may be radiated off the top quark or off the W boson. Figure 4 shows the total cross section for each channel at the Tevatron and at the LHC. These have been calculated using tree-level matrix elements generated by MADGRAPH [32] (and checked against those obtained by COMPHEP [33]) convoluted with the parton distribution function set CTEQ5L [34], with the renormalization[2] and factorization scales set equal to the Higgs boson mass.[3] At the Tevatron, the s-channel process is enhanced by the $p\bar{p}$ initial state and the relatively low machine energy, and its contribution is of the same order of magnitude as that of the t-channel process. In contrast, the t-channel process dominates at the LHC. For the sake of comparison, we have included in Fig. 4 the rates for production of a Higgs boson in association with a $t\bar{t}$ pair.

For intermediate-mass Higgs bosons, $\sigma(th)$ is much smaller than $\sigma(t\bar{t}h)$, their ratio being $\sim 1/10$ at the LHC and $\sim 1/50$ at the Tevatron. This is surprising since the analogous ratio between single top and $t\bar{t}$ production is $\sim 1/2$ at both the LHC and the Tevatron.[4]

It is instructive to pin down the reason for this strong suppression. With this aim we compare in Table I the ratio of the cross sections for single top $\sigma(t)$, and for a $t\bar{t}$ pair $\sigma(t\bar{t})$, with the ratio where the Higgs boson is also produced, $\sigma(th)$ and $\sigma(t\bar{t}h)$. We explicitly single out the contributions from different channels, since their relative importance changes with the collision energy and initial-state particles. Looking at the leading contributions at the LHC (t channel for single top and $gg \to t\bar{t}$) in the first line, we find a suppression factor between the two processes of about $0.33/1.1 \simeq 0.3$. This is due to the destructive interference between the two diagrams in Fig. 1 [22,31].[5] In Fig. 5 we have plotted the relative contributions to the t-channel cross section from each of the two diagrams in Fig. 1, as a function of the Higgs boson mass, at the Tevatron and at the LHC. At the LHC, for a Higgs boson mass of 115 GeV, the cross section due to each diagram alone is $\simeq 3.5$ times larger than the complete cross section, while, for larger Higgs boson masses, the W-Higgs boson contribution becomes dominant.[6] To further support

[2]The renormalization scale is relevant only for the W-associated process.

[3]In the t-channel process, the factorization scale of the light-quark distribution function should actually be the virtuality of the W boson [35]. However, it happens that this makes little difference numerically.

[4]As mentioned in the Introduction, the theoretical prediction for the ratio $\sigma(t)/\sigma(t\bar{t})$ at the Tevatron and the LHC is $\sim 1/3$, when calculated at next-to-leading order in the strong coupling [29,30]. However, since our results for associated production of a Higgs boson plus a single top are only at the tree level, we compare quantities evaluated at the lowest order.

[5]The separation of the amplitude into contributions coming from the Higgs boson coupling to the top quark and to the W is gauge invariant. In the unitary gauge this corresponds to considering the two diagrams in Fig. 1 independently.

[6]This diagram contains a term proportional to the Higgs boson mass itself, as can be seen by calculating the contribution coming from the exchange of a longitudinal W in the t channel. It is exactly this term that dominates the amplitude at large Higgs boson masses.

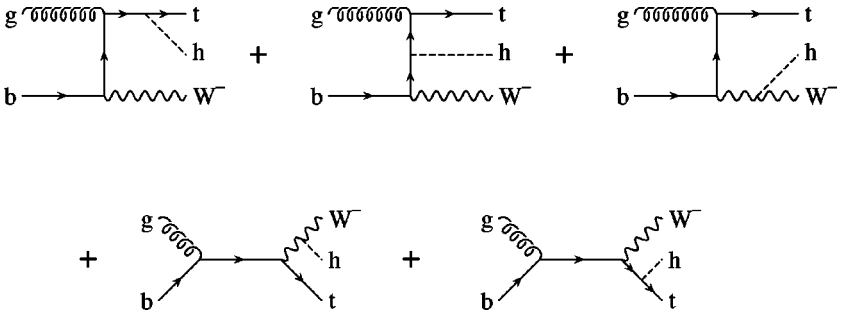

FIG. 3. Feynman diagrams contributing to the *W*-associated production of a Higgs boson plus a single top quark.

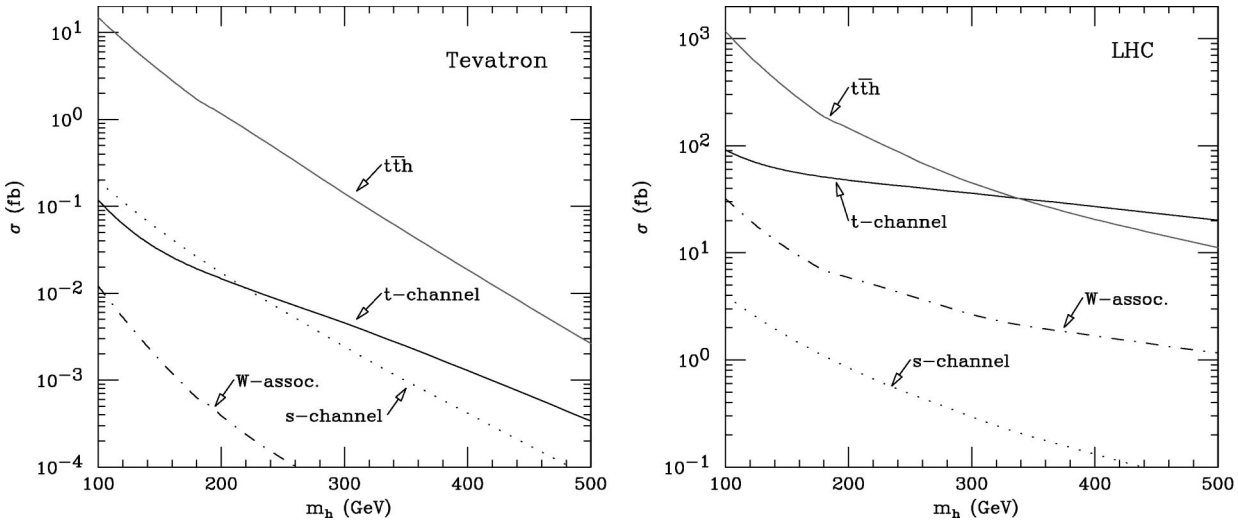

FIG. 4. Cross sections for production of a Higgs boson plus a single top quark at the Tevatron ($p\bar{p}, \sqrt{s}=2$ TeV) and at the LHC ($pp, \sqrt{s}=14$ TeV). Cross sections for the *t*-channel, *s*-channel, and *W*-associated processes are shown. For comparison, the cross section for $t\bar{t}h$ is also shown. The set of parton distribution functions is CTEQ5L, and the renormalization and factorization scales are set equal to the Higgs boson mass.

TABLE I. Comparison of the ratios $\sigma(th)/\sigma(t)$ and $\sigma(t\bar{t}h)/\sigma(t\bar{t})$, for a Higgs boson of mass $m_h = 115$ GeV, at the LHC and at the Tevatron. The set of parton distribution functions is CTEQ5L, and the renormalization and factorization scales are set equal to the top-quark mass in the *t* and $t\bar{t}$ production and to the Higgs-boson mass in the associated processes. All results are leading order. In the second and fourth line, "*t*–Higgs-boson only" means that only the contribution where the Higgs boson couples to the top (first diagram in Figs. 1 and 2) is included in the calculation of $\sigma(th)$.

		$\sigma(th)/\sigma(t)\times 10^3$		$\sigma(t\bar{t}h)/\sigma(t\bar{t})\times 10^3$	
		t ch	*s* ch	gg	$q\bar{q}$
LHC		0.33	0.42	1.1	3.1
	t–Higgs-boson only	1.1	0.28		
Tevatron		0.038	0.20	0.26	1.6
	t–Higgs-boson only	0.21	0.14		

this argument, we have included the contributions to $\sigma(th)$ coming from only the first diagram in Fig. 1 in the second and fourth lines of Table I. Comparing again the ratio $\sigma(th)/\sigma(t)$ in the t channel with the gg contribution to $\sigma(\bar{t}th)/\sigma(t\bar{t})$ at the LHC, we find that they are the same (1.1×10^{-3}). Hence the suppression factor of about 0.3, which we found before, is accounted for by the destructive interference. The same argument applies at the Tevatron $(0.21\times10^{-3}\simeq0.26\times10^{-3})$, where the destructive interference is somewhat stronger than at the LHC (0.038/0.21 $\simeq$0.18) (Fig. 5).

As can be seen from Fig. 5, the reduction of the cross section due to this interference effect strongly depends on the mass of the Higgs boson. In this respect the large suppression found for Higgs boson masses less than 200 GeV can be regarded as a numerical accident. On the other hand, the fact that the interference is destructive is a consequence of unitarity [22]. The simplest way to show this it to recall that at high energies one can describe the t-channel process in the so-called effective-W approximation [36,37], where the initial light quark emits a W, which may be treated as if it is on shell. In so doing the diagram can be factorized into a distribution function of the W in the initial quark times a $2\rightarrow2$ subprocess $Wb\rightarrow ht$. One can show that at high energies E, with $s\sim-t\sim-u\sim E^2\gg m_h^2,m_W^2,m_t^2$, each of the two subdiagrams in Fig. 1 behaves like

$$\mathcal{A}^{t,W}_{\mathrm{t-ch}}\sim g^2\frac{m_tE}{m_W^2}, \tag{1}$$

for an external longitudinal W, where the superscripts t and W indicate from which particle the Higgs boson is radiated. For a $2\rightarrow2$ process, unitarity demands that the total amplitude approaches, at most, a constant, and therefore the terms in Eq. (1) would violate unitarity at a scale $\Lambda\simeq m_W^2/m_tg^2$. However, the unitarity-violating terms in the two amplitudes have opposite signs and cancel when the two diagrams are added. We conclude that although the amount of the suppression depends on the parameters describing the process (such as the top mass, the Higgs boson mass, and the center-of-mass energy), the sign of the interference term is a fundamental property of the Higgs boson sector of the standard model. Moreover, we expect that in extensions of the standard model where unitarity is respected up to arbitrarily high scales, similar cancellations take place. As an example, we have considered the t-channel production in a generic two-Higgs-doublet model (2HDM) and explicitly verified that the terms that grow with energy cancel. The details are presented in Appendix A.

There is a similar explanation of the cancellation between diagrams in the W-associated production. At high energies the two gauge-invariant classes of amplitudes, $\mathcal{A}^t$ and $\mathcal{A}^W$, behave like

$$\mathcal{A}^{t,W}_{W-\mathrm{assoc.}}\sim g_sg^2\frac{m_t}{m_W^2} \tag{2}$$

for an external longitudinal W. Since for a $2\rightarrow3$ process, unitarity demands that the total amplitude decreases as $1/E$, a violation would occur at the scale $m_W^2/m_tg^2g_s$. We explicitly verified that the terms in Eq. (2) cancel when the amplitudes are added together. In the s-channel process, where the interference is constructive, the W always has a large timelike virtuality and the diagrams do not contain any divergent behavior with energy. The interference in the s-channel and W-associated processes is demonstrated in Fig. 6.

III. *t*-CHANNEL PRODUCTION AT THE LHC

In this section we discuss whether a signal for the Higgs boson plus single-top process can be disentangled from the backgrounds. As we have seen in the previous section, the cross section at the Tevatron is far too small to be relevant and therefore we do not investigate it any further. Here we focus on production at the LHC, and in particular on the

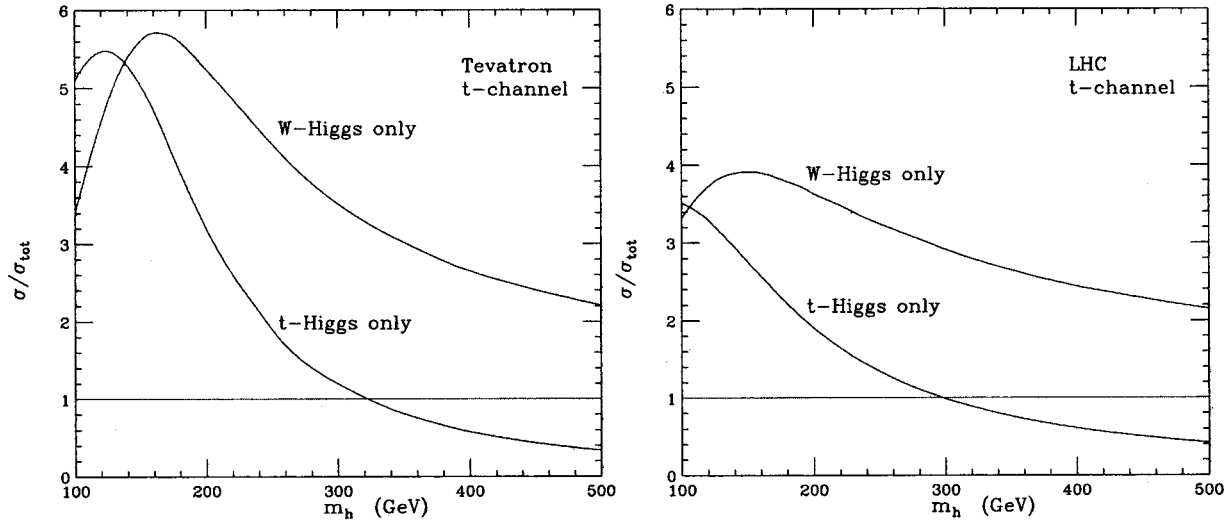

FIG. 5. Interference in the t-channel process at the Tevatron and at the LHC. The contributions from the t-Higgs boson coupling only and the W-Higgs boson coupling only, normalized to the total cross section at any given Higgs boson mass, are shown.

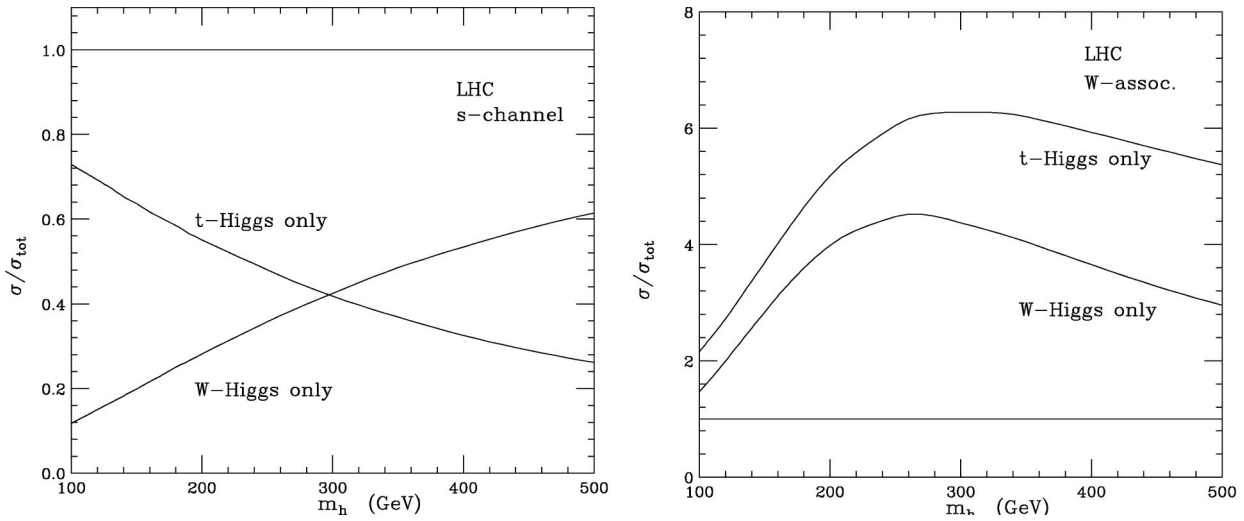

FIG. 6. Interference in the *s*-channel (left) and in the *W*-associated channel (right) at the LHC. The contributions from the *t*-Higgs boson coupling only or *W*-Higgs boson coupling only, normalized to the total cross section at any given Higgs boson mass, are shown.

t-channel process, which is the dominant contribution. All signal and background cross sections are calculated using MADGRAPH [32].

Since the total cross section turns out to be small, detecting any rare decay of the Higgs boson, such as $h\to\gamma\gamma$ [whose branching ratio is $\mathcal{O}(10^{-3})$], as suggested in earlier studies [20–22], is certainly not feasible. It remains to be seen whether the dominant decay modes of a light Higgs boson offer any viable signature. In Fig. 7 we show the total cross section times the branching ratio for $h\to b\bar{b}$ and $h\to W^+W^-$ (calculated using HDECAY [38]) at the Tevatron and at the LHC. The decay into $b\bar{b}$ pairs decreases very quickly and becomes negligible around Higgs boson masses of 160 GeV, exactly where the decay into W^+W^- reaches its maximum. Since the most challenging mass region for the Higgs boson discovery at the LHC is for $m_h\lesssim 130$ GeV, we focus our attention on the Higgs boson decay into $b\bar{b}$ and fix the Higgs boson mass to a nominal value of 115 GeV.

We start by presenting the salient kinematic characteristics of the signal, where the Higgs boson is required to decay to $b\bar{b}$ and the top to decay semileptonically ($t\to bl^+\nu$) to provide a hard lepton trigger and to avoid QCD backgrounds (Fig. 8). We treat the top decay exactly, including spin and width effects. As in the previous section, we have chosen the CTEQ5L set of parton distribution functions and fixed the factorization scale equal to m_h.

In Fig. 9 we show the rapidity distributions of the final-state particles in the signal events. Both the b's from the Higgs boson decay and the b and the lepton from the top decay are produced centrally while the light quark emitting the virtual W favors large rapidities, peaking at around 3 units. The presence of a forward jet is related to the behavior of the cross section as a function of the virtuality of the W boson exchanged in the t channel, $d\sigma/dq^2\sim 1/(q^2-M_W^2)^2$.

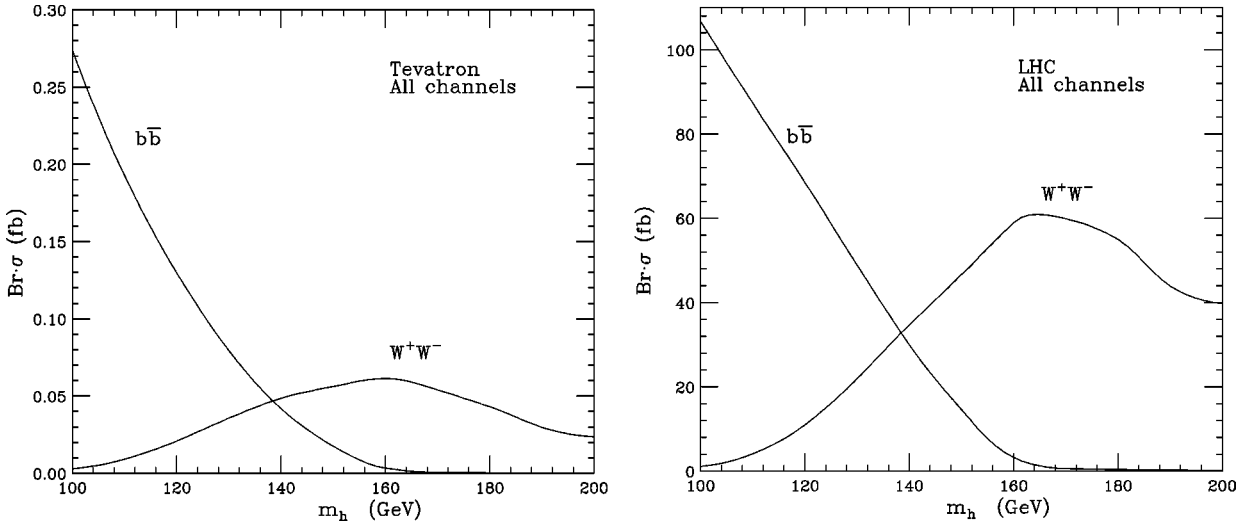

FIG. 7. th cross section times the branching ratio of $h\to b\bar{b}$ and $h\to W^+W^-$ at the Tevatron and at the LHC. The set of parton distribution functions is CTEQ5L, and the renormalization and factorization scales are set equal to the Higgs boson mass.

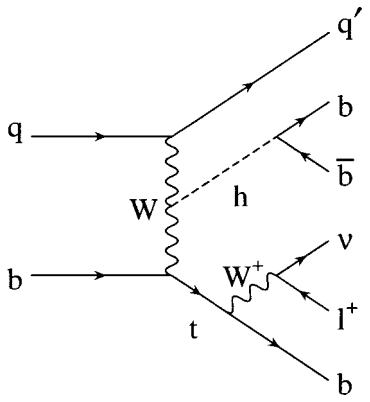

FIG. 8. Example of a Feynman diagram contributing to the signal with three b tags. The final-state particles are explicitly shown.

The region $-q^2 \leqslant M_W^2$ dominates, in analogy to single top production [23–25]. Since we also assume that the charge of the b jet is not measured, the signature for this processes is

$$3b + 1\text{fwd jet} + l^{\pm} + \not{p}^T. \tag{3}$$

In order to estimate the number of events in the detector, we have chosen the acceptances as shown in Table II, corresponding to low-luminosity running ($\mathcal{L} = 10^{33}/\text{cm}^2/\text{s}$). With 30 fb^{-1} we expect around 120 events. When the b-tagging efficiency ($\epsilon_b = 60\%$) and lepton efficiency ($\epsilon_l = 90\%$) are included, the number of expected events goes down to 23.[7] Although the final tally is low, this is more than half of the number of events expected for the $t\bar{t}h$ process after branching ratios and reconstruction efficiencies are taken into account [30]. However, the impact of the backgrounds is more severe for a Higgs boson plus a single top, as we discuss in the following.

The largest sources of irreducible background are from single top production in association with a $b\bar{b}$ pair, coming either from the resonant production of a Z boson (tZ) or from a higher-order QCD process, such as the emission of a gluon subsequently splitting into a $b\bar{b}$ pair ($tb\bar{b}$). Although the final-state particles in the above processes are exactly the same as in the signal, the typical invariant mass $m_{b\bar{b}}$ of the b's in the final state is quite different. Let us study the idealized case where the t is reconstructed with 100% efficiency, such that we know which b comes from top decay. For tZ the distribution in $m_{b\bar{b}}$ is peaked around the Z mass, while for $tb\bar{b}$ it is largest at small invariant mass. We require that the invariant mass of the $b\bar{b}$ pair lies in a window $m_h \pm 2\sigma$, where $\sigma = 11$ GeV is the expected experimental resolution [7]. Assuming a Gaussian distribution, we estimate that 40% of the events coming from tZ fall in this range (for $m_h = 115$ GeV), decreasing quickly for larger Higgs boson masses. The cross sections for the signal and these two irreducible backgrounds are given in Table III with the cut on the invariant mass of the $b\bar{b}$ applied (second row). We see that the backgrounds are comparable to the signal after this cut.

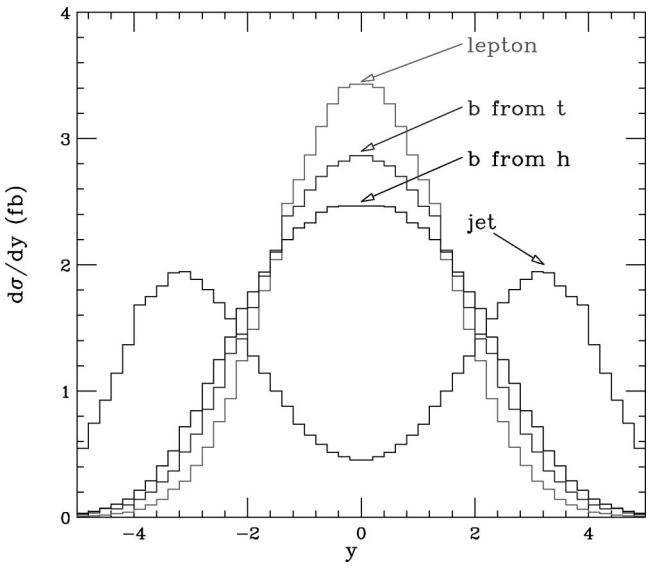

FIG. 9. Rapidity distributions for the final-state particles (the lepton and the b from the top quark, the b's from the Higgs boson, and the jet) in the t channel at the LHC.

An important reducible background comes from the production of a $t\bar{t}$ pair [with $t\bar{t} \to (W^+ \to l^+\nu)(W^- \to c\bar{s})b\bar{b}$], as shown in Fig. 10(a) (fourth column of Table III).[8] This process contributes to the background when the c quark coming from the hadronic decay of one of the W's is misidentified as a b quark and the s quark is the forward jet. A mistag probability $\epsilon_c = 10\%$ is included in the cross sections quoted in Table III.[9] Even in the idealized case where one top quark is reconstructed with 100% efficiency, the number of background events is very large. This background is drastically reduced by requiring the presence of the forward jet (third row of Table III), but it is still large compared with the signal. To reduce this background further one can exploit the fact that the forward jet and the bc that fake the Higgs boson signal all come from top decay, so their invariant mass is nominally 175 GeV. We therefore require that the invariant mass of the forward jet and the $b\bar{b}$ pair exceed 250 GeV (fourth column of Table III). This essentially eliminates the $t\bar{t}$ background,[10] while maintaining most of the signal.

There is a related background, $t\bar{t}j$ [shown in Fig. 10(b)], of which one cannot so easily dispose (fifth column of Table III). In this case the amplitude is dominated by the exchange of a gluon in the t channel and the jet is naturally produced

[7]The efficiencies are taken from Ref. [7].

[8]Other sources of reducible background come from the production of a W in association with four jets of which three are (or are misidentified as) b quarks.

[9]The mistag probability quoted in Ref. [7] is $\epsilon_c = 14\%$, but no specific effort was made to minimize it. We assume that it can be reduced to 10% while maintaining high b-tagging efficiency.

[10]In actuality some of the background will pass the cut due to jet resolution.

TABLE II. Cuts applied to the *t*-channel signal at the LHC (low luminosity), with three and four *b* tags, for $m_h = 115$ GeV. The values of the cross sections after the cuts are applied are shown in the last two columns. Branching ratios $\mathrm{Br}(h \to b\bar{b}) = 77\%$ as well as $\mathrm{Br}(W \to l\nu) = 22\%$ are included. Detector efficiencies are not included.

Cut	$p_b^T >$	$p_{l,\nu}^T >$	$p_j^T >$	$\lvert\eta_{b,l}\rvert <$	$\lvert\eta_j\rvert <$	$\Delta R_{ij} >$	σ_{3b}	σ_{4b}
Value	15 GeV	20 GeV	30 GeV	2.5	5	0.4	4.0 fb	1.9 fb

forward, while both top quarks remain central. If the *s*-quark jet is missed ($P^T < 15$ GeV), the distributions of the remaining particles (the *b*'s, the mistagged *c* quark, and the lepton) are very similar to the ones in Fig. 9. After all cuts are applied, the number of background events is large compared with the signal. We conclude that at the LHC the measurement of the Higgs boson plus single top with three *b* tags is hampered by the overwhelming $t\bar{t}j$ background.

Another possibility for reducing the background is to consider four *b* tags (see Fig. 11). Since the *b* distribution in the proton sea arises from the splitting of virtual gluons into collinear $b\bar{b}$ pairs, the additional *b* tends to reside at small p^T. However, sometimes, this additional *b* will be at high p^T and be detected. Studies performed on single top production have shown that the $p_{\min}^T > 15$ GeV needed at the LHC to detect a jet is enough for the perturbative calculation to be reliable [29]. The $4b$-tag case can be analyzed as above. When detector acceptance is taken into account, the cross section is around one-half of the $3b$-tag one (last column in Table II). Both irreducible and reducible backgrounds are present. The irreducible backgrounds are analogous to tZ and $tb\bar{b}$ discussed in the $3b$-tag case, where an additional *b* present in the final state (arising, as in the signal, from an initial gluon splitting into $b\bar{b}$) is also detected. We again assume that the top quark is reconstructed with 100% efficiency, leaving three pairs of *b*'s in the final state that could have come from Higgs boson decay. We give in Table IV the cross sections with detector cuts and with the requirement that the invariant mass of at least one $b\bar{b}$ pair lies in a window $m_h \pm 22$ GeV. A forward jet cut is added in the third row of Table IV, and also a requirement that the minimum invariant mass of all $b\bar{b}$ pairs (excluding the *b* from top decay) exceed 90 GeV in the fourth row. This last cut reduces the $tb\bar{b}(b)$ background, because the $b\bar{b}$ pair, which comes from gluon splitting, tends to reside at low invariant mass. After all cuts, the irreducible backgrounds are comparable to the signal.

There are several reducible backgrounds to consider, all with top pairs in the final state. We give in the fourth column of Table IV the cross section for $t\bar{t}b\bar{b}$. This process contributes through the decay $t\bar{t}b\bar{b} \to W^+W^-b\bar{b}b\bar{b}$, where one *W* decays hadronically to two jets, one of which is identified as the forward jet while the second is missed (Fig. 12). The forward jet cut and the minimum $b\bar{b}$ mass cut reduce this background to the same level as the signal. A related background, given in the fifth column of Table IV, occurs when the hadronically decaying *W* yields a (mistagged) charm quark. Of the remaining quarks (one *s* and three *b*'s), either the *s* or one of the *b*'s provides the forward jet, and one is missed. The cuts similarly reduce this background to the same level as the signal. There is also a background from $t\bar{t}j$, where the hadronically decaying *W* yields a *c* and *s* quark, both of which are mistagged ($\epsilon_s = 1\%$). This back-

TABLE III. Cross sections (fb) for the signal and some of the most important backgrounds for the Higgs boson plus single-top production in the *t* channel at the LHC (low luminosity), with three *b* tags, for $m_h = 115$ GeV. Branching ratios into final states are included, as well as the *b*-tagging efficiency $\epsilon_b = 60\%$ and the lepton-tagging efficiency $\epsilon_l = 90\%$. The backgrounds include both the irreducible ones (tZ and $tb\bar{b}$) and the reducible ones ($t\bar{t}$ and $t\bar{t}j$). In the reducible backgrounds, a *c* quark from the decay of a *W* is mistagged as a *b* quark (the mistag probability, $\epsilon_c = 10\%$, is included). "Detector cuts" correspond to the choice of cuts in Table II. In the second line, assuming the top is correctly reconstructed, the invariant mass of the other two *b*'s is required to be in a window of $m_h \pm 22$ GeV (95% of the signal and 40% of the tZ background is assumed to fall in this range). In the third line, a forward jet tag is added. In the fourth line a minimum invariant mass of 250 GeV for the Higgs boson candidate and the forward jet is required. The last line gives the expected number of events with 30 fb^{-1} of integrated luminosity at the LHC.

	$3b$ tag (low luminosity)				
	Signal	tZ	$tb\bar{b}$	$t\bar{t}$	$t\bar{t}j$
Detector cuts	0.80	2.1	4.1	810	100
$\lvert m_{b\bar{b}} - m_h\rvert < 22$ GeV	0.75	0.83	0.54	450	38
$\lvert\eta_j\rvert > 2$, $p_j^T > 50$ GeV	0.39	0.44	0.26	13	8.0
$m_{b\bar{b}j} > 250$ GeV	0.35	0.35	0.25		7.4
Events with 30 fb^{-1}	10	10	7		220

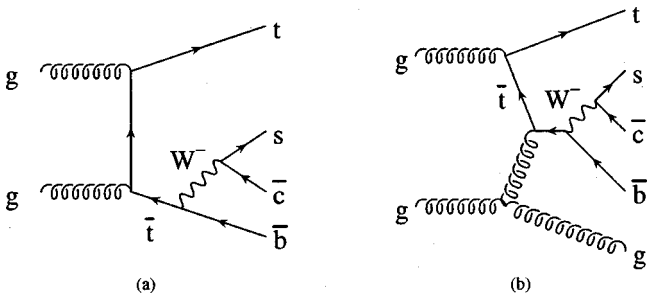

FIG. 10. Reducible backgrounds in the $3b$-tag analysis coming from the production of a $t\bar{t}$ pair and jets. The c quark coming from the decay of a W is misidentified as a b quark. In $t\bar{t}$ production (a) the s quark is the forward jet while in $t\bar{t}j$ production (b) the s-quark jet is missed.

ground is the largest of all, but it is removed by the requirement on the minimum $b\bar{b}$ invariant, since the (mistagged) cs pair comes from W decay.[11]

Although each background in the $4b$-tag analysis is comparable to the signal, there are only a few signal events with 30 fb^{-1}. Therefore, there is little hope of observing a signal in this channel, unless significantly more than 30 fb^{-1} can be delivered while maintaining the same detector performance. At high luminosity ($\mathcal{L}=10^{34}/\text{cm}^2/\text{s}$), it is anticipated that the minimum p_T for jets must be raised to 30 GeV. In Table V we study the signal and backgrounds in this scenario (the b-tagging efficiency is also lowered to 50%). After all cuts, the $t\bar{t}b\bar{b}$ backgrounds are now each twice as large as the signal, because these backgrounds involve missing a jet, which is more likely with the increased jet p_T threshold. The number of signal events in 300 fb^{-1} is about 10, with about 55 background events. Significantly more integrated luminosity would be needed to see a signal in this channel.

IV. PRODUCTION OF SUPERSYMMETRIC HIGGS BOSONS

It is interesting to ask whether there could be an enhancement in the signal when the production of nonminimal Higgs bosons is considered. With this aim we have investigated the production of a light CP-even (h) and a CP-odd (A) Higgs boson in the MSSM.

The Higgs boson sector of the MSSM is the same as the 2HDM presented in Appendix A except that it depends (at tree level) on only two free parameters, which can be chosen to be m_A and $\tan\beta$. The tree-level relations between the Higgs boson masses are modified by radiative corrections that involve the supersymmetric particle spectrum, mainly of the top sector [3–5]. Since the analytical form of the corrections is quite involved (see Ref. [39]) we used HDECAY [38] to evaluate the Higgs boson masses and the mixing parameter α, given m_A, $\tan\beta$, and information on the top-squark mixings and masses.

[11]In actuality, some of this background will remain due to jet resolution.

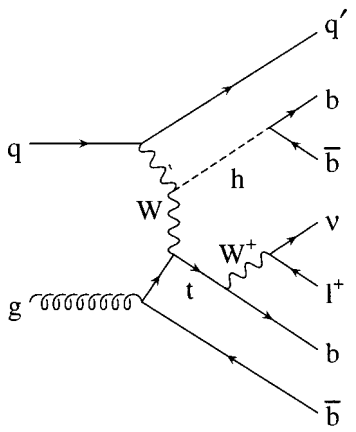

FIG. 11. Example of a Feynman diagram contributing to the signal in the $4b$-tag analysis.

For large m_A, the masses of the heavy Higgs bosons approximately coincide, $m_A \simeq m_H \simeq m_{H^\pm}$, while the CP-even Higgs boson remains light. This is the so-called decoupling limit, where the standard-model couplings and particle content are recovered. In the case of large $\tan\beta$ and small m_A, one finds that $m_h \simeq m_A$ and the Higgs boson couplings to the vector bosons and to the fermions are different from those predicted by the standard model. In particular, there is a strong enhancement of the bottom-quark coupling to both the h and the A, which can give rise to interesting signatures at the colliders [6,40–42]. We focus our attention in this area of the parameter space, which is not excluded by the measurements from the CERN e^+e^- collider LEP [2], choosing $m_A<120$ GeV and $10<\tan\beta<50$.

In Fig. 13 we show the cross section for production of the CP-even Higgs boson h and CP-odd Higgs boson A in association with single top as a function of m_A and $\tan\beta$. These are calculated using tree-level matrix elements generated by MADGRAPH [32] (and checked against those obtained by COMPHEP [33]) convoluted with the parton distribution function set CTEQ5L [34], and with the renormalization and factorization scales set equal to the Higgs boson mass. We assume a simplified scenario where the third generation diagonal soft-supersymmetry-breaking squark masses are degenerate, with a common value $M_{\text{SUSY}}=1$ TeV, and the mixing between the top squarks maximal, $X_t=A_t-\mu\cot\beta=\sqrt{6}M_{\text{SUSY}}$, with $\mu=-200$ GeV (for an extensive discussion on the other possible choices, see Ref. [6] and references therein).

As shown in Fig. 13, for $\tan\beta\gtrsim 30$, the cross sections are indeed enhanced with respect to that for a standard-model Higgs boson. However, the increase is never very large. This is basically due to two reasons. First, from the arguments presented in Sec. II and Appendix A, unitarity imposes large cancellations among the various diagrams, even in the MSSM Higgs boson sector. In this respect, the production of the CP-odd state A is particularly instructive. Because of its CP quantum numbers, this state cannot couple to two W's and therefore the contribution from the second diagram in Fig. 1 vanishes. One might guess that the destructive inter-

TABLE IV. Cross sections (fb) for the signal and some of the most important backgrounds for the Higgs boson plus single top production in the t channel at the LHC (low luminosity), with four b tags, for $m_h = 115$ GeV. Branching ratios into final states are included, as well as the b-tagging efficiency $\epsilon_b = 60\%$ and the lepton-tagging efficiency $\epsilon_l = 90\%$. The backgrounds include both the irreducible ones [$tZ(b)$ and $tb\bar{b}(b)$] and the reducible ones [$t\bar{t}b\bar{b}$, $t\bar{t}b\bar{b}$ (mistag), $t\bar{t}j$]. In $t\bar{t}b\bar{b}$ (mistag) and $t\bar{t}j$, a c quark from the decay of a W is mistagged as a b quark (the mistag probability, $\epsilon_c = 10\%$, is included); in $t\bar{t}j$, an s quark from the decay of a W is mistagged (the mistag probability, $\epsilon_s = 1\%$, is included). "Detector cuts" correspond to the choice of cuts in Table II. In the second line, assuming the top is correctly reconstructed, the invariant mass of at least one pair of the other three b's is required to be in a window of $m_h \pm 22$ GeV (95% of the signal and 40% of the tZ background is assumed to fall in this range). In the third line, a forward jet tag is added. In the fourth line a minimum invariant mass of 90 GeV for all $b\bar{b}$ pairs (not including the b that reconstructs the top quark) is required. The last line gives the expected number of events with 30 fb^{-1} of integrated luminosity at the LHC.

		$4b$-tag (low luminosity)				
	Signal	$tZ(b)$	$tb\bar{b}(b)$	$t\bar{t}b\bar{b}$	$t\bar{t}b\bar{b}$ (mistag)	$t\bar{t}j$
Detector cuts	0.22	0.42	1.5	5.8	3.1	9.0
$\lvert m_{b\bar{b}} - m_h \rvert < 22$ GeV	0.21	0.17	0.61	2.6	2.3	6.3
$\lvert \eta_j \rvert > 2$	0.15	0.11	0.41	0.17	0.18	2.4
$\min m_{b\bar{b}} > 90$ GeV	0.1	0.065	0.08	0.053	0.078	
Events with 30 fb^{-1}	3.0	1.9	2.5	1.6	2.3	

ference with the diagrams where A couples to the quarks cannot take place anymore and the signal could be much larger. In fact, the complete calculation shows that the diagram where the A couples to the W and a charged Higgs boson H^+ (see the second diagram in Fig. 14) provides the terms that cancel the large (and unitarity-violating) contributions coming from the other diagrams (Appendix A). Second, the effects due to the choice of a large value of $\tan\beta$ work in opposite directions for the bottom and the top quark, leading to an enhancement of the coupling of the Higgs boson to the bottom quark but to a suppression for the top quark. As a result the rates for the h and the A are comparable to that of a standard-model Higgs boson with a similar mass for $m_b \tan\beta \approx m_t$. For instance, taking $m_h = m_A = 115$ GeV and $\tan\beta = 50$, we have $\sigma(th) \simeq \sigma(tA) = 190$ fb, which is 2.5 times the cross section expected in the standard model. Considering the production of the two Higgs bosons together,[12] it would be possible to achieve a significance $S/\sqrt{B} \simeq 5$ in the $4b$-tag analyses (see Tables IV and V).

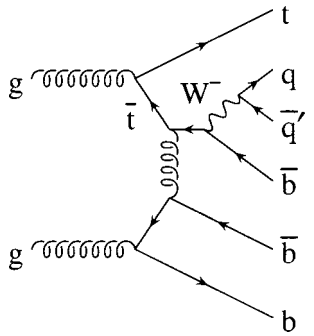

FIG. 12. Reducible background in the $4b$-tag analysis coming from the production of $t\bar{t}b\bar{b}$. One of the quarks coming from the W is missed while the other provides the forward tag.

V. CONCLUSIONS

In this paper we revisited the production of the Higgs boson in association with single top at hadron colliders. We provided the full set of cross sections at both the Tevatron and the LHC for the three production processes (t channel, s channel and W associated) and we investigated in some detail why they are smaller than what one would expect compared with $t\bar{t}h$ production. For the t channel, which gives the most important contribution at the LHC, this is due to large cancellations taking place between different diagrams. We have shown that the above peculiarity is not accidental but is a consequence of the renormalizability of theory, and we gave a detailed proof in the general framework of a two-Higgs-doublet model.

Focusing on the t-channel process, we discussed the possibility of detecting the production of Higgs boson plus single top at the LHC, concentrating on the decay of the Higgs boson into $b\bar{b}$. We considered events where three and four b quarks are tagged. In the case of three b tags, there is an overwhelming background from $t\bar{t}j$. In the case of four b tags there is no single overwhelming background, but rather several backgrounds that are comparable to the signal. Given our present expectations for detector capabilities and luminosity at the LHC, it seems unlikely that one can extract a signal from the backgrounds.

There are several things that could improve this progno-

[12]There is no interference between the two processes due to the different CP properties of the Higgs bosons.

TABLE V. Cross sections (fb) for the signal and some of the most important backgrounds for the Higgs boson plus single top production in the t-channel at the LHC (high luminosity), with four b-tags, for $m_h = 115$ GeV. Branching ratios into final states are included, as well as the b-tagging efficiency $\epsilon_b = 50\%$ and the lepton-tagging efficiency $\epsilon_l = 90\%$. The backgrounds include both the irreducible ones [$tZ(b)$ and $tb\bar{b}(b)$] and the reducible ones [$t\bar{t}b\bar{b}$, $t\bar{t}b\bar{b}$ (mistag), $t\bar{t}j$]. In $t\bar{t}b\bar{b}$ (mistag) and $t\bar{t}j$, a c quark from the decay of a W is mistagged as a b quark (the mistag probability, $\epsilon_c = 10\%$, is included); in $t\bar{t}j$, an s quark from the decay of a W is mistagged (the mistag probability, $\epsilon_s = 1\%$, is included). "Detector cuts" correspond to the choice of cuts in Table II, apart from the minimum p_b^T, which is now raised to 30 GeV. In the second line, assuming the top is correctly reconstructed, the invariant mass of at least one pair of the other three b's is required to be in a window of $m_h \pm 22$ GeV (95% of the signal and 40% of the tZ background is assumed to fall in this range). In the third line, a forward jet tag is added. In the fourth line a minimum invariant mass of 90 GeV for all $b\bar{b}$ pairs (not including the b that reconstructs the top quark) is required. The last line gives the expected number of events with 300 fb^{-1} of integrated luminosity at the LHC.

		4b-tag (high luminosity)				
	Signal	$tZ(b)$	$tb\bar{b}(b)$	$t\bar{t}b\bar{b}$	$t\bar{t}b\bar{b}$ (mistag)	$t\bar{t}j$
Detector cuts	0.061	0.094	0.23	4.0	1.5	3.3
$\lvert m_{b\bar{b}} - m_h \rvert < 22$ GeV	0.058	0.037	0.096	1.7	1.1	2.5
$\lvert \eta_j \rvert > 2$	0.040	0.025	0.067	0.15	0.11	0.94
$\min m_{b\bar{b}} > 90$ GeV	0.032	0.018	0.027	0.069	0.068	
Events with 300 fb^{-1}	9.5	5.5	8.0	21	21	

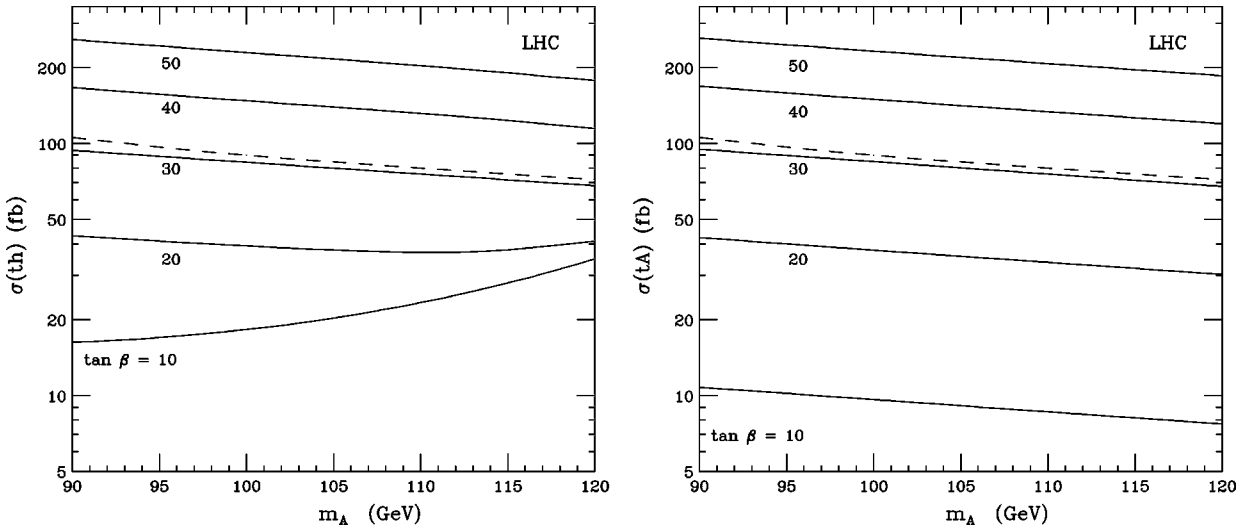

FIG. 13. Cross sections for production of a CP-even Higgs boson h and a CP-odd Higgs boson A in association with a single top as a function of m_A and $\tan\beta$ ($M_{\rm SUSY} = 1$ TeV, $\mu = -200$ GeV and maximal top-squark mixing is assumed). Only t-channel production is included. The cross section for a standard-model Higgs boson with $m_{h_{\rm SM}} = m_A$ is given as a reference (dashes). The set of parton distribution functions is CTEQ5L and the factorization scale is set equal to the Higgs boson mass.

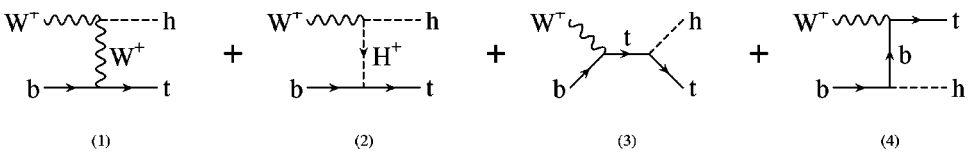

FIG. 14. Diagrams contributing to $W^+ b \to h\, t$ in the 2HDM.

sis. Several of the backgrounds involve a mistagged c quark, and if the mistag rate can be reduced significantly below 10%, these backgrounds would be less severe. One might also be able to find a more efficient set of cuts to reduce the backgrounds. Since the signal involves the t-channel exchange of a W boson, one might be able to use a rapidity gap to distinguish the signal from the reducible backgrounds (the irreducible backgrounds also involve t-channel W exchange, however) [43].

Finally we have also presented the results for the t-channel production of the CP-even state h and the CP-odd state A of the MSSM at the LHC. For $m_A<120$ GeV and large $\tan\beta$ there is a moderate enhancement of the production rate compared to that of a standard-model Higgs boson, which may be enough to disentangle the signal from the QCD backgrounds.

ACKNOWLEDGMENTS

We are grateful for correspondence with D. Froidevaux, J. Incandela, S. Kuhlmann, E. Ros, and A. Rozanov regarding charm mistagging. This work was supported in part by the U. S. Department of Energy under Contract No. DOE DE-FG02-91ER40677. We gratefully acknowledge the support of GAANN, under Grant No. DE-P200A980724, from the U.S. Department of Education for K.P.

APPENDIX A

In this appendix, we consider the case of t-channel production in a generic 2HDM. Using the effective-W approximation, we show that the amplitudes represented by the diagrams in Fig. 14 contain terms that grow with energy. Nevertheless, the unitarity of the model implies that these terms must cancel in the final result, as we show explicitly. In a generic 2HDM that is invariant under $SU(2)_L\times U(1)_Y$ and conserves CP, the scalar fields $\Phi_{1,2}$ are doublets of $SU(2)_L$ with hypercharge $Y=1/2$, and they develop vacuum expectation values $v_{1,2}$ that break $SU(2)_L\times U(1)_Y$ to $U(1)_{\rm EM}$. This results in a mass $m_W^2=\frac{1}{4}g^2v^2$ and $m_Z^2=\frac{1}{4}(g^2+g'^2)v^2$ with $v^2=v_1^2+v_2^2=(\sqrt{2}G_F)^{-1}$. The particle content can be exploited to fully parametrize the model. In addition to $\tan\beta=v_2/v_1$, we can use the masses of the four scalars $h,H,A,H^{\pm}$, the mixing angle α between the CP-even states h,H, and one of the couplings appearing in the quartic potential. The inclusion of the fermions must be done with care in order to suppress tree-level flavor-changing neutral currents. One common choice is to impose a discrete symmetry in such a way that Φ_1 couples only to down-type quarks and leptons, while Φ_2 couples only to up-type quarks [44]. This way of coupling the Higgs boson fields to the fermions is the same as in the minimal supersymmetric standard model and is called type II.

The contributions from the four diagrams in Fig. 14 read

$$i\mathcal{A}_1=i\frac{gg_{WWh}m_W}{2\sqrt{2}}\overline{u}(p_t)\gamma^{\mu}(1-\gamma^5)u(p_b)\times\frac{g_{\mu\nu}-[(p_b-p_t)_{\mu}(p_b-p_t)_{\nu}]/m_W^2}{(p_b-p_t)^2-m_W^2}\epsilon_W^{\nu}, \tag{A1}$$

$$i\mathcal{A}_2=i\frac{gg_{WH^+h}}{2\sqrt{2}}\overline{u}(p_t)\left[\frac{m_t}{m_W}\cot\beta(1-\gamma^5)+\frac{m_b}{m_W}\tan\beta\times(1+\gamma^5)\right]u(p_b)\frac{\epsilon_W(p_t-p_b-p_h)}{(p_b-p_t)^2-m_{H^+}^2}, \tag{A2}$$

$$i\mathcal{A}_3=-i\frac{gg_{tth}}{2\sqrt{2}}\frac{\overline{u}(p_t)(\not{p}_t+\not{p}_h+m_t)\not{\epsilon}_W(1-\gamma^5)u(p_b)}{(p_t+p_h)^2-m_t^2}, \tag{A3}$$

$$i\mathcal{A}_4=-i\frac{gg_{bbh}}{2\sqrt{2}}\frac{\overline{u}(p_t)\not{\epsilon}_W(1-\gamma^5)(\not{p}_b-\not{p}_h+m_b)u(p_b)}{(p_b-p_h)^2-m_b^2}, \tag{A4}$$

which in the high-energy limit $(s,-t,-u\gg m_h^2,m_{H^+}^2,m_W^2,m_t^2)$ and for a longitudinally-polarized W $(\epsilon_W^{\mu}\simeq p_W^{\mu}/m_W)$ reduce to

$$i\mathcal{A}_1\sim i\frac{gg_{WWh}}{4\sqrt{2}\,m_W^2}\overline{u}(p_t)[m_b(1+\gamma^5)-m_t(1-\gamma^5)]u(p_b), \tag{A5}$$

$$i\mathcal{A}_2\sim i\frac{gg_{WH^+h}}{2\sqrt{2}\,m_W^2}\overline{u}(p_t)[m_b\tan\beta(1+\gamma^5)+m_t\cot\beta(1-\gamma^5)]u(p_b), \tag{A6}$$

$$i\mathcal{A}_3\sim -i\frac{gg_{tth}}{2\sqrt{2}\,m_W}\overline{u}(p_t)(1-\gamma^5)u(p_b), \tag{A7}$$

$$i\mathcal{A}_4\sim i\frac{gg_{bbh}}{2\sqrt{2}\,m_W}\overline{u}(p_t)(1+\gamma^5)u(p_b). \tag{A8}$$

Unitarity therefore requires that the following relations hold true:

$$\frac{g_{WWh}}{2}m_b+g_{WH^+h}\tan\beta m_b+g_{bbh}m_W=0, \tag{A9}$$

$$-\frac{g_{WWh}}{2}m_t+g_{WH^+h}\cot\beta m_t-g_{tth}m_W=0. \tag{A10}$$

That this is indeed the case can be easily verified using the couplings of the 2HDM,

$$g_{WWh}=g\sin(\beta-\alpha), \tag{A11}$$

$$g_{WH^+h}=-\frac{g}{2}\cos(\beta-\alpha), \tag{A12}$$

$$g_{tth}=-\frac{gm_t}{2m_W}\frac{\cos\alpha}{\sin\beta}, \tag{A13}$$

$$g_{bbh}=\frac{gm_b}{2m_W}\frac{\sin\alpha}{\cos\beta}. \tag{A14}$$

Analogous relations can be derived for the production of the heavy neutral Higgs boson H and the results can be obtained from those above with the replacement $\alpha \to \alpha - \pi/2$. The production of the CP-odd state A differs from that of the CP-even Higgs bosons in that its coupling to the W boson is zero. In this case the divergent terms coming from the diagrams where the Higgs boson couples to the quarks, cancel with those coming from the second diagram in Fig. 14. An explicit calculation gives

$$i\mathcal{A}_2 \sim \frac{g g_{WH^+A}}{2\sqrt{2}\, m_W^2} \overline{u}(p_t)[m_b \tan\beta(1+\gamma^5) + m_t \cot\beta(1-\gamma^5)]u(p_b), \tag{A15}$$

$$i\mathcal{A}_3 \sim -\frac{g g_{ttA}}{2\sqrt{2}\, m_W} \overline{u}(p_t)(1-\gamma^5)u(p_b), \tag{A16}$$

$$i\mathcal{A}_4 \sim -\frac{g g_{bbA}}{2\sqrt{2}\, m_W} \overline{u}(p_t)(1+\gamma^5)u(p_b). \tag{A17}$$

Unitarity entails that

$$g_{WH^+A} \tan\beta m_b + g_{bbh} m_W = 0, \tag{A18}$$

$$g_{WH^+A} \cot\beta m_t + g_{tth} m_W = 0. \tag{A19}$$

The above constraints are satisfied by the couplings of the 2HDM,

$$g_{WH^+A} = \frac{g}{2}, \tag{A20}$$

$$g_{ttA} = -\frac{g m_t}{2 m_W} \cot\beta, \tag{A21}$$

$$g_{bbA} = -\frac{g m_b}{2 m_W} \tan\beta. \tag{A22}$$

[1] M. Luscher and P. Weisz, Phys. Lett. B **212**, 472 (1988).
[2] LEP Electroweak Working Group, CERN-EP-2000-016.
[3] H.E. Haber and R. Hempfling, Phys. Rev. Lett. **66**, 1815 (1991).
[4] Y. Okada, M. Yamaguchi, and T. Yanagida, Prog. Theor. Phys. **85**, 1 (1991).
[5] J. Ellis, G. Ridolfi, and F. Zwirner, Phys. Lett. B **257**, 83 (1991).
[6] M. Carena *et al.*, hep-ph/0010338.
[7] CMS Collaboration, Technical Proposal, CERN/LHCC/94-38 (1994); ATLAS Collaboration, Technical Design Report, CERN/LHCC/99-15 (1999).
[8] S.L. Glashow, D.V. Nanopoulos, and A. Yildiz, Phys. Rev. D **18**, 1724 (1978).
[9] J.N. Ng and P. Zakarauskas, Phys. Rev. D **29**, 876 (1984).
[10] Z. Kunszt, Nucl. Phys. **B247**, 339 (1984).
[11] R. Kleiss, Z. Kunszt, and W.J. Stirling, Phys. Lett. B **253**, 269 (1991).
[12] W.J. Marciano and F.E. Paige, Phys. Rev. Lett. **66**, 2433 (1991).
[13] J.F. Gunion, Phys. Lett. B **261**, 510 (1991).
[14] J.F. Gunion, P. Kalyniak, M. Soldate, and P. Galison, Phys. Rev. Lett. **54**, 1226 (1985).
[15] A. Stange, W. Marciano, and S. Willenbrock, Phys. Rev. D **49**, 1354 (1994).
[16] A. Stange, W. Marciano, and S. Willenbrock, Phys. Rev. D **50**, 4491 (1994).
[17] J. Dai, J.F. Gunion, and R. Vega, Phys. Rev. Lett. **71**, 2699 (1993).
[18] J. Goldstein, C.S. Hill, J. Incandela, S. Parke, D. Rainwater, and D. Stuart, Phys. Rev. Lett. **86**, 1694 (2001).
[19] J.L. Diaz-Cruz and O.A. Sampayo, Phys. Lett. B **276**, 211 (1992).
[20] W.J. Stirling and D.J. Summers, Phys. Lett. B **283**, 411 (1992).
[21] A. Ballestrero and E. Maina, Phys. Lett. B **299**, 312 (1993).
[22] G. Bordes and B. van Eijk, Phys. Lett. B **299**, 315 (1993).
[23] S.S. Willenbrock and D.A. Dicus, Phys. Rev. D **34**, 155 (1986).
[24] C.P. Yuan, Phys. Rev. D **41**, 42 (1990).
[25] R.K. Ellis and S. Parke, Phys. Rev. D **46**, 3785 (1992).
[26] S. Cortese and R. Petronzio, Phys. Lett. B **253**, 494 (1991).
[27] T. Stelzer and S. Willenbrock, Phys. Lett. B **357**, 125 (1995).
[28] A.P. Heinson, A.S. Belyaev, and E.E. Boos, Phys. Rev. D **56**, 3114 (1997).
[29] T. Stelzer, Z. Sullivan, and S. Willenbrock, Phys. Rev. D **58**, 094021 (1998).
[30] M. Beneke *et al.*, in ''Proceedings of the Workshop on Standard Model Physics (and more) at the LHC,'' CERN Yellow Report, CERN-2000-04; M. Beneke *et al.*, hep-ph/0003033.
[31] T. Tait and C.P. Yuan, Phys. Rev. D **63**, 014018 (2001).
[32] T. Stelzer and W.F. Long, Comput. Phys. Commun. **81**, 357 (1994).
[33] A. Pukhov *et al.*, hep-ph/9908288.
[34] H.L. Lai *et al.*, Phys. Rev. D **51**, 4763 (1995); hep-ph/9410404.
[35] T. Stelzer, Z. Sullivan, and S. Willenbrock, Phys. Rev. D **56**, 5919 (1997).
[36] S. Dawson, Nucl. Phys. **B249**, 42 (1985).
[37] Z. Kunszt and D.E. Soper, Nucl. Phys. **B296**, 253 (1988).
[38] A. Djouadi, J. Kalinowski, and M. Spira, Comput. Phys. Commun. **108**, 56 (1998).
[39] H.E. Haber, R. Hempfling, and A.H. Hoang, Z. Phys. C **75**, 539 (1997).
[40] D.A. Dicus and S. Willenbrock, Phys. Rev. D **39**, 751 (1989).
[41] J. Dai, J.F. Gunion, and R. Vega, Phys. Lett. B **345**, 29 (1995).
[42] J. Dai, J.F. Gunion, and R. Vega, Phys. Lett. B **387**, 801 (1996).
[43] D. Rainwater, R. Szalapski, and D. Zeppenfeld, Phys. Rev. D **54**, 6680 (1996).
[44] S.L. Glashow and S. Weinberg, Phys. Rev. D **15**, 1958 (1977).